Electronic Supplementary Information

Gelation of metal oxide cluster for proton exchange membrane operated under low humidity

Xinpei Li[a], Qiang Yu[b], Kun Chen[b], Linkun Cai[b], Lu Liu[b], Mingxin Zhang[c], Yuan Liu[b], Yijie Gu[a]*, Jia-Fu Yin[b]*, Panchao Yin[b]*

[a] *School of Machinery and Automation, Weifang University, Weifang 261000, China.*
[b] *State Key Laboratory of Luminescent Materials and Devices & South China Advanced Institute for Soft Matter Science and Technology, South China University of Technology, Guangzhou 510640, China.*
[c] *State Key Laboratory of Marine Resource Utilization in South China Sea, School of Chemical Engineering and Technology, Hainan University, Haikou 570228, China.*

1. Materials and methods

1.1 Chemicals and material preparations

1.1.1 Chemicals

PVA-203, PVA-124 and PVA-224 were purchased from shanghai Titan Scientific Co., Ltd. $H_3[PW_{12}O_{40}]$, glycerol and H_3BO_3 were purchased from Aladdin company and used as received. Deionized water was obtained from the Millipore ultra-pure water system in all reactions.

1.1.2 Gel preparations

A certain amount of glycerol, $H_3[PW_{12}O_{40}]$, PVA, and H_3BO_3 were homogeneously dissolved in deionized water to form a solution. The solution was then stirred at 60 °C for 12 h in a vial to obtain the resultant products.

1.2 Characterization techniques

1.2.1 Contact angle

The membranes were adhered to an acetone-cleaned glass plate and then, different droplets of water, formamide and diiodomethane were laid on the surface of membranes. The contact angle was measured by the sessile drop method using the contact angle test device (OCA40 Micro, Germany).

Table S1 Surface free energy parameters for different liquids

Liquid	γ_L/mN/m	γ_L^{LW}/mN/m	γ_L^+/mN/m	γ_L^-/mN/m
Water	72.8	21.8	25.5	25.5
Formamide	58.0	39.0	2.28	39.6
Diiodomethane	50.8	50.8	0	0

According to extended Young equation (1) and (2) listed below, the surface tension of solid (γ_S) can be afforded:

$$(\gamma_L^{LW} + 2\sqrt{\gamma_L^+ \gamma_L^-})(1-\cos\theta) = 2(\sqrt{\gamma_S^{Lw} \gamma_L^{LW}} + \sqrt{\gamma_S^+ \gamma_L^-} + \sqrt{\gamma_S^- \gamma_L^+}) \quad (1)$$

$$\gamma_S = \gamma_S^{Lw} + 2\sqrt{\gamma_S^+ \gamma_S^-} \quad (2)$$

Abbreviation:

θ: Young contact angle (°);

γ_L: surface free energy of liquid (mN/m);

γ_L^{LW}: LW interfacial tension of liquid (mN/m);

γ_L^+: acceptor (Lewis acid) surface parameter of liquid (mN/m);

γ_L^-: donor (Lewis base) surface parameter of liquid (mN/m);

γ_S: surface free energy of solid (mN/m);

γ_S^{LW}: LW interfacial tension of solid (mN/m);

γ_S^+: acceptor (Lewis acid) surface parameter of solid (mN/m);

γ_S^-: donor (Lewis base) surface parameter of solid (mN/m).

1.2.2 Water-holding capacity Stability

Gravimetric analyses were carried out at RT daily for 90 days, where the relative humidity is controlled by dehumidifier (Parkoo, YDA-8138EB). Thermal analyses were performed on a TGA 5500 from TA instruments.

1.2.3 Mechanical performance evaluation

Uniaxial tensile testing data was recorded on a universal tensile instrument (LABSANS LD22. 102). The sample was processed into dumbbell-shape specimen, then, the afforded specimen was stretched with constant speed of 8 mm/min until fracture. The engineering stress (σ) was calculated based on $\sigma = F/A_0$, where F is the applied force and A0 is the original cross-sectional area of the dumbbell-shape sample. The engineering strain (ε) was determined by $\varepsilon = (L - L_0)/L_0 \times 100\%$, where L and L_0 are the length during stretching and the initial gauge length of the sample, respectively. The toughness was calculated by integrating the area under the engineering stress-strain curve.

1.2.4 Rheology measurement protocol

The sample was processed into circular film with diameter of 25 mm. The rheological amplitude sweep and small amplitude oscillatory shearing data was recorded on a stress-controlled rheometer (Anton Paar MCR302 rheometer equipped with a temperature controlling system). The diameter of the parallel-plate geometry was 25 mm.

1.2.5 Broadband dielectric spectroscopy (BDS)

BDS experiments were carried out on a Novocontrol Concept 80 system with an Alpha-ANB impedance analyzer and a Quatro Cryo-system temperature system. The accessible frequency in single measurement ranges from 10-1 Hz to 107 Hz at selected temperature (193.15 K to 353.15 K, the step was set to be 10 K). During the test, samples were put into a sandwich-type cell with diameter of 11 mm and thickness of 5.5 mm.

1.2.6. Scanning electron microscopy

The solvent of the gel sample was removed under vacuum. Before the test, the sample was treated with gold sputtering. Then, the microscopic morphologies of the samples were probed by using Hitachi Regulus 8100 scanning electron microscopy (SEM) instruments. Energy dispersive X-ray (EDX) analysis was conducted to identify the chemical compositions of the samples.

1.2.7 Small angle X-ray scattering (SAXS)

The microstructures of the hydrogel were characterized on home-lab X-ray scattering equipment (Rigaku). The samples were mounted in the beamline hutch and exposed to a Cu Kα X-ray beam with wavelength of 1.54 Å. The scattered X-ray was recorded by using Hypix-6000 detector to obtain the light intensity plot as a function of scattering vector q (0.08 to 4 $Å^{-1}$). The scattering vector is reciprocal to the spatial length and is given by $q= 4\pi Sin\theta/\lambda$, where λ is wavelength of the X-ray beam, 2θ is the scattering angle. The background scattering data from the Kapton film was recorded and subtracted for each sample. The scattering data were analyzed on Irena (APS, X-ray science division) and Igor Pro (WaveMetrics, OR) platform.

1.2.8 Raman spectroscopy

Raman spectroscopy was conducted with fiber optic Raman system with BWS 785 nm beam laser, Rayleigh line cutoff at 150 cm^{-1}, high quantum efficiency CCD array detector.

1.2.9 X-ray diffraction (XRD)

The XRD measurement was carried out by the Rigaku SmartLab SE diffractometer with HyPix-400 2D detector, copper rotating anode (Cu Kα X-ray), and Bragg Brentano parafocusing optics and parallel beam optics with a parabolic X-ray mirror.

1.3 Fuel cell device assembly and operation

Membrane electrode assembly (MEA) was fabricated by sandwiching MOC-based membranes with two gas diffusion electrodes (4 cm^2 of geometric area). The MEA was mounted in a single cell composed of two carbon plates with ribbed channels for supplying gases. The current-voltage (I-V) polarization curves were recorded by a single cell test at 30 °C under the dry gas (hydrogen and oxygen). The flow rate of hydrogen and oxygen was fixed at 100 mL/min. The backpressure was atmospheric pressure.

2. Discussions on the effects of the stoichiometry of glycerol, H_3PW_{12}, PVA-203 and H_3BO_3

As for the gel electrolytes applicable for the use in the fuel cell device, balanced proton conductivity and mechanical properties are needed. Show in Table S2 below, a series of controlled experiments show that appropriate stoichiometric ratios critical for affording high performance gel electrolyte. Inside the gels, PVA component contributes to the enhancement of the mechanical performance, while PW_{12} serves as proton donors. By fine-tuning the stoichiometric ratios of different components, GHPH-1 with satisfactory mechanical property and proton conductivity is therefore afforded, which is further used in fuel cell devices in our research work.

3. Supplemented Figures and tables

Table S2 Recipes for different samples

Components / Samples	*Glycerol*	*H_3PW_{12}*	*PVA-203*	*H_3BO_3*	*σ (S/cm) ×10^{-3}*
GHPH-2	3 g	3 g	1.5 g	1.5 g	2.74
GHPH-3	3 g	2 g	2 g	1.5 g	3.54
GHPH-4	3 g	1 g	1 g	1.5 g	0.978
GHPH-5	3 g	3.5 g	1.5 g	1.5 g	4.90
GHPH-6	3 g	2 g	1 g	1.5 g	1.47
GHPH-7	3 g	1.5 g	0.5 g	1.5 g	0.287
GHPH-8	3 g	1 g	1.5 g	1.5 g	2.07
GHPH-9	3 g	1.5 g	1.5 g	1.5 g	3.29

GHPH-10	3 g	2 g	1.5 g	1.5 g	3.29
GHPH-11	3 g	2 g	2 g	1.5 g	3.60
GHPH-1	3 g	2 g	3 g	1.5 g	5.80
HP	None	2 g	3 g	None	0.14
GHP	3 g	2 g	3 g	None	0.913
GHPH-12	3 g	4.0 g	3 g	1.5 g	3.30
GHH	3 g	2 g	None	1.5 g	2.60
GPH	3 g	None	3 g	1.5 g	1.60

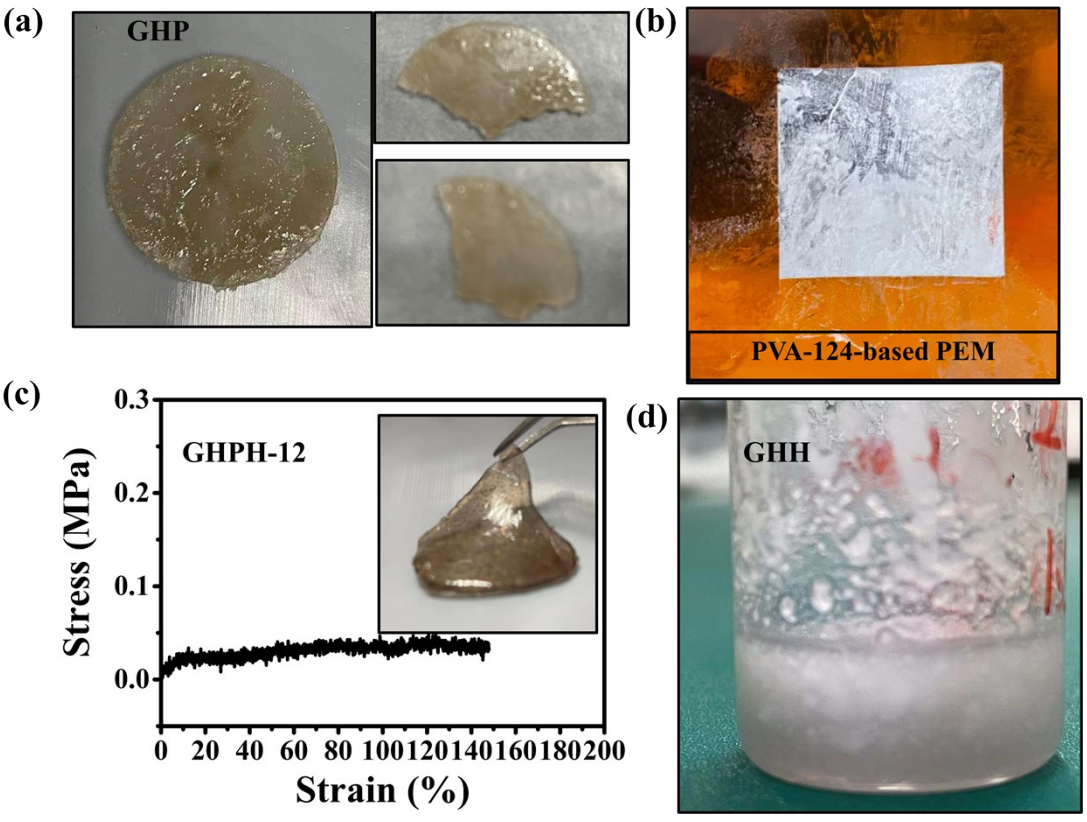

Fig. S1 (a) The visualized images for GHP; (b) Membranes for PVA-124-based PEM; (c) Tensile

stress-strain curves for GHPH-12 and the inset is the visualized images of GHPH-12; (d) The visualized images for GHH.

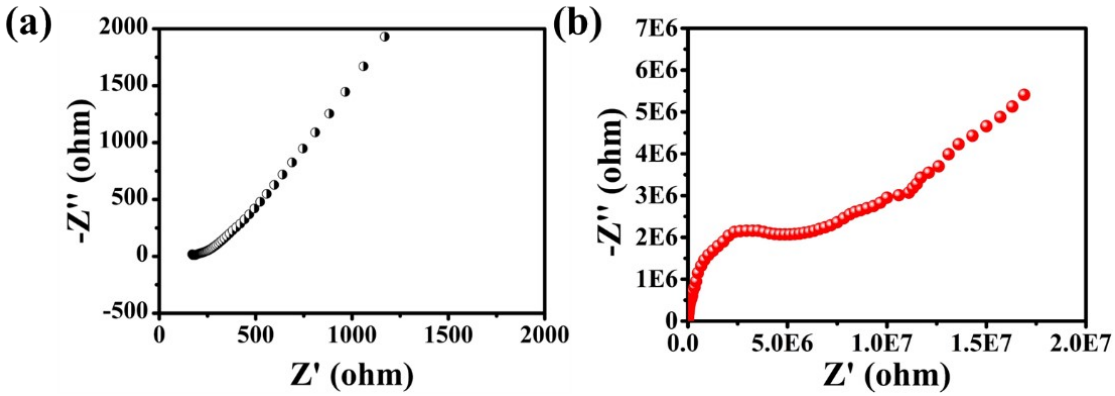

Fig. S2 EIS spectra of GHPH-1 and PVA-224-based GE.

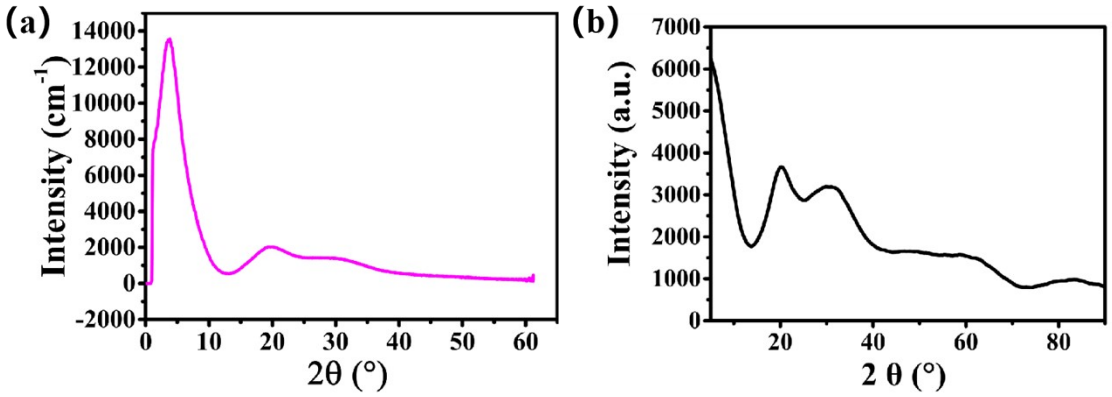

Fig. S3 (a) SAXS data of GHPH-1. (b) SAXS data of GHPH-1 (2θ versus intensity).

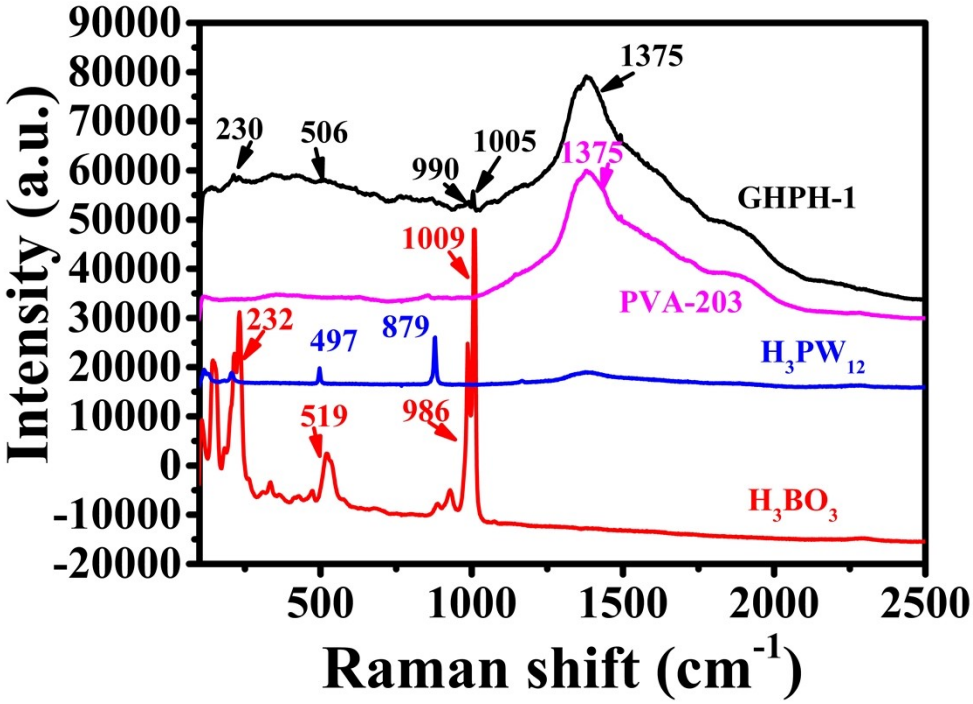

Fig. S4 Raman spectra of GHPH-1, PVA-203, H_3PW_{12} and H_3BO_3.

Table S3 Swelling rate of GHPH-1 at different RH.

	Length (mm)	*Width (mm)*	*Weight (g)*
52% RH; RT	6.5	3.1	0.0204
98% RHT=35°C	6.5	3.1	0.0285
Swelling ratio (%)	0	0	39.7

Abbreviation: RH: Relative Humidity; RT: Room Temperature

Table S4 Summary for the conductivities of GHPH-1 at different RH

Samples	*Temperature (°C)*	*Humidity (%)*	*Conductivity (s/cm) × 10⁻³*
GHPH-1	30	30	0.47
GHPH-1	30	60	0.59
GHPH-1	30	70	1.30

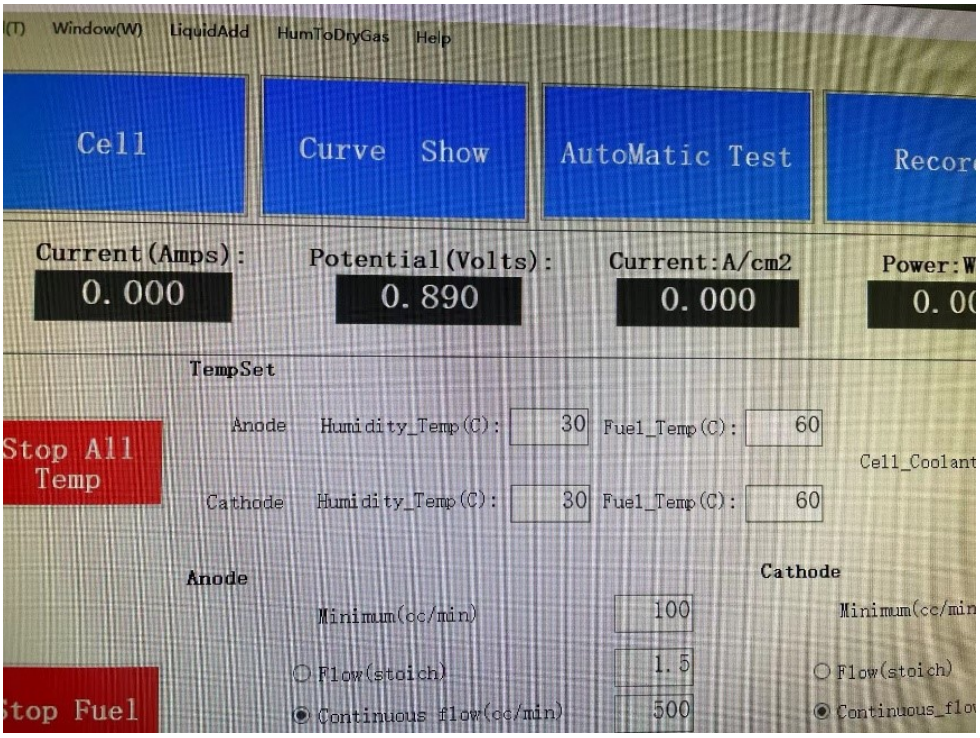

Fig. S5 Open circuit voltage for the assembled electrode.